**Proceedings of the ASME 2010 International Design Engineering Technical Conferences &
Computers and Information in Engineering Conference
IDETC/CIE 2010
August 15-18, 2010, Montreal, Quebec, Canada**

DETC2010-28189

A ROBUST SOLUTION OF THE SPHERICAL BURMESTER PROBLEM

Jorge Angeles
Department of Mechanical Engineering
McGill University, Montreal, Canada
e-mail: angeles@cim.mcgill.ca

Shaoping Bai*
Department of Mechanical and Manufacturing Engineering
Aalborg University, Denmark
e-mail: shb@me.aau.dk

ABSTRACT

The problem of spherical four-bar linkage synthesis is revisited in this paper. The work is aimed at developing a robust synthesis method by taking into account both the formulation and the solution method. In addition, the synthesis of linkages with spherical prismatic joints is considered by treating them as a special case of the linkages under study. A two-step synthesis method is developed, which sequentially deals with equation-solving by a semigraphical approach and branching-detection. Examples are included to demonstrate the proposed method.

1 Introduction

The synthesis of spherical four-bar linkages is a classic problem that has been extensively studied in the literature [1–4]. This paper focuses on the problem of *motion synthesis*, a.k.a. *synthesis for rigid-body guidance*, whereby a discrete set of orientations is to be visited by the coupler link of a spherical four-bar linkage. This problem is also known as the *Spherical Burmester Problem*.

Essentially, the synthesis of spherical four-bar linkages leads to a system of trigonometric equations. Different solution methods have been reported in the literature on the subject. A method to robustly select intermediate orientations for motion generators was proposed by Widyan and Angeles [5]. The kinematic mapping was applied to the synthesis problem, as reported by Brunnthaler et al. [6].

To some extent, the spherical Burmester problem can be considered as an extension of the classic planar Burmester problem and hence, paraphrasing Burmester [7], stated as '*Are there any spherical four-bar mechanisms whose coupler link can visit four or five prescribed orientations* ?' The solution of the synthesis problem hinges on two issues: the formulation of the problem and its solution. We emphasize robustness in both the formulation and the solution. The formulation must be general and include particular cases, i.e., cases with Ball points.

In this paper, we aim to develop a comprehensive synthesis method by addressing the robustness of both the formulation and the solution method. A semigraphical approach is adopted, which eases the detection of real solutions. In this method, the synthesis equations are converted into a system of bi-variate equations, and hence, can be readily visualized. Upon identification of the real solutions, a numerical solver is adopted for the accurate calculation of the solutions. This approach has been applied by the authors to the planar Burmester problem. The work reported here is a natural extension of the authors' previous work [8].

2 Problem Formulation

The spherical four-bar linkage under study is depicted in Fig. 1, with its four linkage dimensions $\{\alpha_j\}_1^4$. The two grounded revolutes are labelled B and B^*, the points at which their axes intersect the unit sphere, the two moving revolutes A and $A^\star$, the points at which their axes intersect the same sphere. Let the reference positions of the moving revolutes be A_0 and $A_0^\star$, the linkage then being fully defined by the two

*Address all correspondence to this author.

Copyright © 2010 by ASME

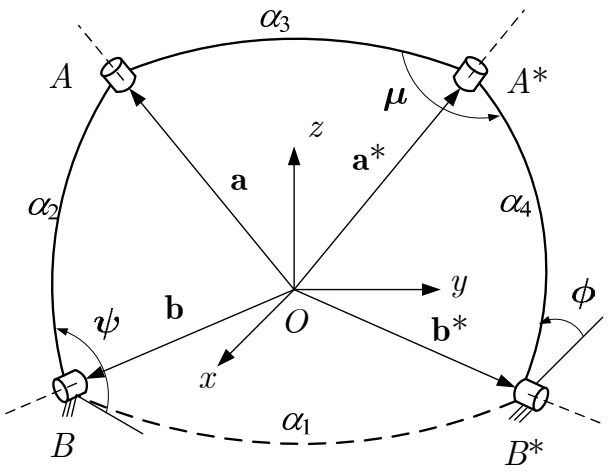

FIGURE 1. The spherical 4R linkage

dyads BA_0 and $B^\star A_0^\star$. By analogy with the planar Burmester problem, points B and $B^\star$ are called *centerpoints*, while A_0 and $A_0^\star$ *circlepoints*. As the coupler link moves, while visiting the m given attitudes of the coupler link, the circlepoint, which is common to both the grounded link $\widehat{BA}$ and the coupler link, attains positions $A_1, \ldots, A_m$, the segments along the axis of the moving revolute of the dyad thus becoming $\overline{OA}_1, \ldots, \overline{OA}_m$, as shown in Fig. 2. The axes of the revolutes of one dyad are thus given by the segments $\overline{OB}$ and $\overline{OA}_0$; the position vectors of B and A_0 are $\mathbf{b}$ and $\mathbf{a}_0$, both of unit magnitude, i.e.,

$$\|\mathbf{b}\| = 1, \quad \|\mathbf{a}_0\| = 1 \tag{1}$$

Likewise, the position vectors of points $B^\star$ and $A_0^\star$ are denoted by the unit vectors $\mathbf{b}^\star$ and $\mathbf{a}_0^\star$. With the foregoing model, the spherical Burmester problem is stated as:

> *Find a spherical four-bar linkage that will conduct its coupler link through a set $\mathscr{S}$ of m attitudes given by the orthogonal matrices $\{\mathbf{Q}_j\}_1^m$, defined with respect to a reference attitude given by $\mathbf{Q}_0 = \mathbf{1}$, where* $\mathbf{1}$ *denotes the* 3×3 *identity matrix.*

3 Synthesis with m Prescribed Poses

For dyad BA_0, by virtue of the link rigidity, the angle between $\overline{OA}_j$ and $\overline{OB}$ remains constant. The *synthesis equation* is thus obtained upon imposing this geometric constraint, i.e.,

$$\mathbf{a}_j^T\mathbf{b} = \mathbf{a}_0^T\mathbf{b} \quad \text{or} \quad (\mathbf{a}_j - \mathbf{a}_0)^T\mathbf{b} = 0, \quad j = 1, \ldots, m \tag{2}$$

where, apparently,

$$\mathbf{a}_j = \mathbf{Q}_j\mathbf{a}_0 \tag{3}$$

whence conditions (2) become

$$\mathbf{a}_0^T(\mathbf{Q}_j^T - \mathbf{1})\mathbf{b} = 0, \quad j = 1, \ldots, m \tag{4}$$

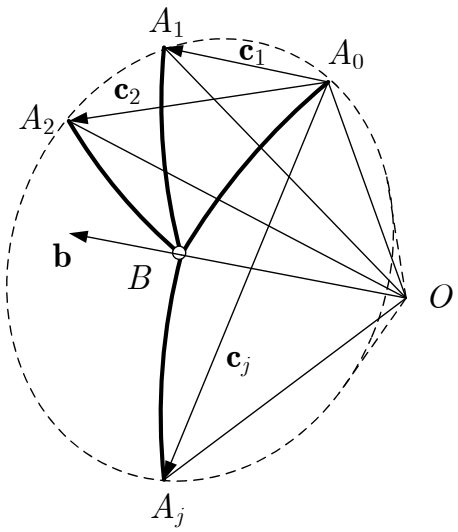

FIGURE 2. A spherical dyad and the conic surface formed by the moving axis OA

In order to ease the ensuing discussion, let

$$\mathbf{c}_j \equiv (\mathbf{Q}_j - \mathbf{1})\mathbf{a}_0 \tag{5}$$

Equation (4) then taking the form

$$\mathbf{c}_j^T\mathbf{b} = 0, \quad j = 1, \ldots, m \tag{6}$$

Geometrically, Eq. (6) states that vector $\mathbf{b}$ is perpendicular to any vector $\mathbf{c}_j$. Referring to Fig. 2, this means that segment $\overline{OB}$ is perpendicular to segments $\overline{A_0A}_j$, $j = 1, \ldots, m$.

Note that the rotation matrices $\mathbf{Q}_j$ admit various parameterizations, the one adopted here is in terms of the *natural invariants* of the rotation [9]. An expression for the rotation matrix $\mathbf{Q}_j$ takes the form

$$\mathbf{Q}_j = \mathbf{1} + s_j\mathbf{E}_j + (1 - c_j)\mathbf{E}_j^2, \quad c_j \equiv \cos\phi_j, \quad s_j \equiv \sin\phi_j \tag{7}$$

where $\mathbf{E}_j$ denotes the *cross-product matrix* (CPM) of $\mathbf{e}_j$, the unit vector that defines the direction of the axis of rotation of

Copyright © 2010 by ASME

$\mathbf{Q}_j$, and ϕ_j the corresponding angle. That is,

$$\mathbf{E}_j = CPM(\mathbf{e}_j) \equiv \frac{\partial(\mathbf{e}_j \times \mathbf{v})}{\partial \mathbf{v}} \tag{8}$$

for any $\mathbf{v} \in \mathbb{R}^3$. Hence,

$$\mathbf{Q}_j - \mathbf{1} = [s_j \mathbf{1} + (1 - c_j)\mathbf{E}_j]\mathbf{E}_j \tag{9}$$

Therefore, Eq.(4) becomes

$$\mathbf{a}_0^T \mathbf{E}_j [s_j \mathbf{1} - (1 - c_j)\mathbf{E}_j]\mathbf{b} = 0, \quad j = 1, \ldots, m \tag{10}$$

which is the *synthesis equation* of the problem at hand. Its solution for various values of m is discussed below.

3.1 Three Poses

In this case, $m = 2$, i.e., two constraint equations occur:

$$\mathbf{c}_1^T \mathbf{b} = 0, \quad \text{and} \quad \mathbf{c}_2^T \mathbf{b} = 0 \tag{11}$$

Hence, one of the two vectors $\mathbf{a}_0$ and $\mathbf{b}$ can be prescribed arbitrarily. If, for example, the former is prescribed, then $\mathbf{c}_1$ and $\mathbf{c}_2$ are known. The conditions of Eq. (11) are thus verified for $\mathbf{b}$ defined as the unit vector derived from the cross product of the two other vectors in the above equations, i.e.,

$$\mathbf{b} = \frac{\mathbf{c}_1 \times \mathbf{c}_2}{\|\mathbf{c}_1 \times \mathbf{c}_2\|} \tag{12}$$

A similar reasoning, with obvious modifications, follows if $\mathbf{b}$ is prescribed.

3.2 Four Poses

Now we have $m = 3$, the constraints being

$$\mathbf{c}_1^T \mathbf{b} = 0, \quad \mathbf{c}_2^T \mathbf{b} = 0 \quad \text{and} \quad \mathbf{c}_3^T \mathbf{b} = 0 \tag{13}$$

In order to be able to find a vector $\mathbf{b}$ simultaneously perpendicular to all three vectors $\mathbf{c}_j$ in the above equation, these three vectors must be coplanar, and hence,

$$F(\mathbf{a}_0) \equiv \mathbf{c}_1 \times \mathbf{c}_2 \cdot \mathbf{c}_3 = 0 \tag{14}$$

which is a product of three factors that are linearly homogeneous in $\mathbf{a}_0$, as per Eq. (5), and hence, it is cubic and homogeneous in $\mathbf{a}_0$. Equation (14) together with the first of equations (1) constitutes the *synthesis equations*, which yield a spherical cubic curve on the unit sphere centered at the origin. Any point on the curve represents a solution of $\mathbf{a}_0$. In light of this, we call the curve the *circlepoint curve*. This curve is, in fact, the *generatrix* of a cubic conical surface $\mathscr{K}$ of apex O.

By a similar reasoning, the *centerpoint conical surface* $\mathscr{M}$ and the *centerpoint curve* are obtained likewise. Any point of the circlepoint curve gives one solution of the centerpoint $\mathbf{b}$.

3.3 Five Poses

For $m = 4$, the synthesis equations lead to a system of four homogeneous bilinear equations in the unknown vectors $\mathbf{a}_0$ and $\mathbf{b}$. As these are three-dimensional vectors, the total number of unknowns at hand is six, but then again, two additional equations are available, namely, Eqs. (1), and the problem is fully determined. The four homogeneous equations can then be cast in the form

$$\underbrace{\begin{bmatrix} \mathbf{a}_0^T \mathbf{E}_1 [s_1 \mathbf{1} - (1 - c_1)\mathbf{E}_1] \\ \mathbf{a}_0^T \mathbf{E}_2 [s_2 \mathbf{1} - (1 - c_2)\mathbf{E}_2] \\ \mathbf{a}_0^T \mathbf{E}_3 [s_3 \mathbf{1} - (1 - c_3)\mathbf{E}_3] \\ \mathbf{a}_0^T \mathbf{E}_4 [s_4 \mathbf{1} - (1 - c_4)\mathbf{E}_4] \end{bmatrix}}_{\equiv \mathbf{C}} \mathbf{b} = \mathbf{0}_4 \tag{15}$$

in which $\mathbf{C}$ is a 4×3 matrix. In light of the second of equations (1), moreover, the trivial solution of eqs.(15) is not acceptable, and hence, $\mathbf{C}$ must be *rank-deficient*, i.e., its three columns must be linearly dependent. This happens if and only if the four independent 3×3 determinants obtained by taking three rows of $\mathbf{C}$ at a time vanish. Let

$$\Delta_j(\mathbf{a}_0) \equiv \det(\mathbf{C}_j) = 0, \quad j = 1, \ldots, 4 \tag{16}$$

with $\mathbf{C}_j$ denoting the 3×3 matrix obtained from $\mathbf{C}$ upon deleting its jth row. From Section 3.2 it is known that each of the four determinants defines a conical cubic surface whose apex is the origin. The common intersections of all four surfaces are common elements of these surfaces; they are the multiple moving-revolute axes that are capable of guiding the coupler link through the five prescribed poses.

Likewise, surface equations for $\mathbf{b}$ can be formulated with

$$\mathbf{D}\mathbf{a}_0 = \mathbf{0}_4 \tag{17}$$

in which the 4×3 matrix $\mathbf{D} = [\mathbf{d}_1, \ldots, \mathbf{d}_4]^T$ with $\mathbf{d}_j = (\mathbf{Q}_j^T - \mathbf{1})\mathbf{b}$, $j = 1, \ldots, 4$. Rank-deficiency of matrix $\mathbf{D}$ yields

$$\Delta_j(\mathbf{b}) \equiv \det(\mathbf{D}_j) = 0, \quad j = 1, \ldots, 4 \tag{18}$$

Copyright © 2010 by ASME

with $\mathbf{D}_j$ denoting the 3×3 matrix obtained from $\mathbf{D}$ upon deleting its jth row.

The Bezout number of the four cubic equations (16) is $3^4 = 81$. Ditto that of the four cubic equations (18). This number is an overestimate of the actual number of possible solutions, which is known to be six [3,4].

As a consequence, the problem admits six, four, two or zero circlepoint solutions. The same reasoning leads to the conclusion that the problem also admits six, four, two or zero centerpoint solutions. Therefore, the number of possible dyads that solve the problem is six, four, two or zero. Correspondingly, the number of spherical four-bar linkages that can guide their coupler link through the five given attitudes is the number of combinations of six, four, two or none objects taking two at a time, i.e., 15, 6, 1 or 0.

4 Synthesis Method for Five Prescribed Attitudes

A synthesis method is developed based on the foregoing principles underlying the spherical Burmester problem. To this end, a semigraphical method is proposed, that filters out the complex solutions.

4.1 A Semigraphical Approach to Equation Solving

We shall use *spherical coordinates* on the unit sphere, namely, *longitude* and *latitude*. Let, then, ϑ_A and φ_A be the longitude and the latitude of A_0, ϑ_B and φ_B those of B. Hence,

$$\mathbf{a}_0 = \begin{bmatrix} \cos\varphi_A \cos\vartheta_A \\ \cos\varphi_A \sin\vartheta_A \\ \sin\varphi_A \end{bmatrix}, \quad \mathbf{b} = \begin{bmatrix} \cos\varphi_B \cos\vartheta_B \\ \cos\varphi_B \sin\vartheta_B \\ \sin\varphi_B \end{bmatrix} \tag{19}$$

As the synthesis equation (4) is homogenous in $\mathbf{a}_0$, both $\mathbf{a}_0$ and $-\mathbf{a}_0$ are solutions to the equation. On the other hand, $\mathbf{a}_0$ and $-\mathbf{a}_0$ define the same axis of rotation from the point of view of a mechanism. Due to this consideration, the ranges of all spherical coordinates are specified as $\{\varphi_A, \vartheta_A, \varphi_B, \vartheta_B\} \in [-\pi/2, \pi/2]$.

Now the four determinant equations (16) in $\mathbf{a}_0$ become equations in the harmonic functions of φ_A and ϑ_A. To solve all four equations robustly, the method used here to compute all real solutions is based on a semigraphical approach: the jth determinant equation (16) defines a contour $\mathscr{C}_j$ in the φ_A-ϑ_A plane. If the four contours are plotted in the rectangle $-\pi/2 \le \varphi_A \le \pi/2$, $-\pi/2 \le \vartheta_A \le \pi/2$, then the intersections of the four contours yield *all the real solutions* sought. As discussed in Section 3.3, there may exist six, four, two or zero real solutions. In the case of zero solutions, no common intersection of the contours appears in the superimposed plots.

The intersections are estimated by inspection on the four contours. These estimates can then further be used as initial guesses in an iterative procedure to yield accurate solutions. The method proposed here to compute the real solutions with an accuracy much higher than their estimates relies on nonlinear least-squares: the four equations (16) in the two unknowns φ_A and ϑ_A can be regarded as an *overdetermined system of nonlinear equations*. Its least-square approximation which, in our case, is their solution, can be most robustly and efficiently obtained with the Newton-Gauss method, as proposed in [10].

Following the same procedure for the computation of $\mathbf{a}_0$, the solutions of $\mathbf{b}$ are found based on the contour equations (18), rather than on the linear homogenous equations (15), in order to avoid roundoff-error propagation.

4.2 Branching-detection

Spherical four-bar linkages, like their planar counterparts, are known to be *bimodal*, which means that, for each value of their input angle, they admit two *assembly modes*. Each mode defines one solution branch of their input-output equation. The coupler link can thus visit attitudes that lie in one of the two branches. If poses of the other branch are to be visited, then the linkage must be disassembled and reassembled in the alternative mode. Branching-defect in the realm of the spherical Burmester problem occurs when the prescribed attitudes lie in different branches of the synthesized linkage. In the presence of four prescribed attitudes, linkages free of branch-defect may be found because of the infinitely many solutions available. In the case of five prescribed attitudes, a discrete set of solutions is available, and hence, each must be verified for branch-defect. If this occurs, then the only alternative to cope with it is by means of a reformulation of the practical problem at hand. If the problem allows for it, then one of the five poses is to be varied, so as to yield a linkage free of branch-defect.

Branch-defect, or *branching* for brevity, can be detected in *planar* four-bar linkages by means of the sign of the sine of the transmission angle [11]. Given the analogy of the properties of the planar linkages with their spherical counterparts, the same criterion applies to the latter. Branching-detection then amounts to sign-detection in the case at hand.

The cosine of the transmission angle of spherical four-bar linkages is known to be given by [4]

$$\cos\mu = \frac{\cos\alpha_3\cos\alpha_4 - \cos\alpha_1\cos\alpha_2 - \sin\alpha_1\sin\alpha_2\cos\psi}{\sin\alpha_3\sin\alpha_4} \tag{20}$$

Correspondingly, the sine of the transmission angle can be found from unit vectors $\mathbf{a}, \mathbf{a}^\star$ and $\mathbf{b}^\star$, introduced in Fig. 1, namely,

$$\sin\mu = \| \bar{\mathbf{a}} \times \bar{\mathbf{b}} \| \,/ (\| \bar{\mathbf{a}} \| \| \bar{\mathbf{b}} \|) \tag{21}$$

Copyright © 2010 by ASME

where $\overline{\mathbf{a}} = \mathbf{a} - (\mathbf{a}\cdot\mathbf{a}^\star)\mathbf{a}^\star$ and $\overline{\mathbf{b}} = \mathbf{b} - (\mathbf{b}\cdot\mathbf{a}^\star)\mathbf{a}^\star$ with $\mathbf{a} = \mathbf{Q}\mathbf{a}_0$, $\mathbf{a}^\star = \mathbf{Q}\mathbf{a}_0^\star$. The sign of the sine of the transmission angle is identical to the following expression

$$f(\mu) = \text{sign}\left[(\overline{\mathbf{a}}\times\overline{\mathbf{b}})\cdot\mathbf{a}^\star\right] \tag{22}$$

5 Spherical Linkages with a P-joint

A spherical linkage may contain a slider moving on a circular guide, similar to the planar crank-slider mechanism. Hence, a spherical linkage may end up with a P-joint[1], where a slider can move along a guiding slot or a guide ring, as illustrated in Example 3. If the guiding slot is fixed, it can be uniquely determined by a unit vector. In turn, the circle is formed by rotating a great arc of 90° about an axis parallel to the unit vector. This axis passes through the origin and a point called *Ball center* [3]. All points on the great circle are called *Ball points*.

A spherical linkage with a P-joint is a special case of the four-bar spherical linkage with $\alpha_4 = 90°$. The foregoing method of synthesis still applies, if with some modifications. If the prescribed attitude leads to a linkage that admits a P-joint, then the circle traced by the centerpoint A, or $A^\star$ for that matter, becomes a major circle. In this case, Eq. (2) becomes

$$\mathbf{b}^T\mathbf{Q}_j\mathbf{a}_0 = 0, \quad j = 0,\ldots,m \tag{23}$$

which can be rewritten as

$$\mathbf{H}\mathbf{a}_0 = \mathbf{0}_n \tag{24}$$

where $\mathbf{H}$ is a $n\times 3$ matrix with $n = m+1$. Again, matrix $\mathbf{H}$ has to be *rank-deficient*. This implies, for the four-pose synthesis problem, that

$$\det(\mathbf{H}_i) = 0, \quad i = 1,\ldots,4 \tag{25}$$

the 3×3 matrix $\mathbf{H}_i$ obtained by removing the ith row from matrix $\mathbf{H}$. In the case of five poses, $\mathbf{H}_i$ is obtained by deleting the ith and $(i+1)$st rows from matrix $\mathbf{H}$.

Following the semigraphical method described in Section 4, we can find $\mathbf{b}$, which is the unit vector defining the P-joint. A similar procedure is applied if the P-joint is the one associated with $B\,(B^\star)$.

[1]A slider that moves on a circular guide was called a *circular prismatic joint* in [12]. We call it simply a P-joint for brevity

TABLE 1. Five poses for Example 1

ϕ_j[rad]	$\mathbf{e}^T$	$[\beta_1,\beta_2,\beta_3]$[deg]
0	[0,0,1]	[0,0,0]
0.2034	$[-0.0449,-0.5133,-0.8569]$	$[-10.0,-6.0,0]$
1.1957	$[0.1827,0.7709,-0.6101]$	$[-51.0,-52.0,-12.0]$
1.1932	$[0.5212,0.8414,-0.1422]$	$[15.0,-56.0,47.0]$
1.0512	$[0.5384,0.8114,0.2271]$	$[33.0,-40.0,47.0]$

6 Examples

We include three examples to demonstrate the application of the method proposed here. All example problems were solved with Maple. Maple's least-square solver `LSSolve` was used for the implementation of the Newton-Gauss method.

6.1 Example 1: Five-Pose Synthesis

In this example, the design task is described by five poses of the coupler link that are to be visited. As listed in Table 1, the orientations are expressed in terms of natural invariants. The corresponding attitude in terms of longitude, latitude and roll angles, β_1, β_2 and β_3, respectively, are also given in the same table, with the purpose of helping the reader visualize the prescribed attitudes.

Figure 3 shows the four contour plots derived from Eq. (16). Four common intersections can be identified for both $\mathbf{a}_0$ and $\mathbf{b}$ from the plots, which imply four sets of real solutions for each vector. Based on the intersections, solutions of $\mathbf{a}_0$ and $\mathbf{b}$ were obtained using Maple's least-square solver `LSSolve`. To match each solution for $\mathbf{a}_0$ and its corresponding solution for $\mathbf{b}$, the linear equations derived from a value of $\mathbf{a}_0$ are used: for example, each solution of $\mathbf{a}_0$ is substituted into the synthesis equation (4), which yields a system of m linear equations in $\mathbf{b}$. The values of $\mathbf{b}$ that verify the linear equations is the one corresponding to the given value of $\mathbf{a}_0$. The matched solutions are recorded in Table 2. Note that the results are also the solutions of vectors $\mathbf{a}_0^\star$ and $\mathbf{b}^\star$. Six linkages, shown in Fig. 4, can thus be generated from the four dyads.

Branching-detection on the six mechanism was conducted with Eq. (22). Sign change of the sine of the transmission angle was found with mechanisms M3 and M4, which indicates the presence of branch-defect in these two mechanisms. The remaining mechanisms were found free of branch-defect. Our mechanism animations further confirmed this point. It was also found from animations that mechanisms M1, M2 and M5 are of the crank-rocker type, while mechanism M6 is of the double-rocker type.

Copyright © 2010 by ASME

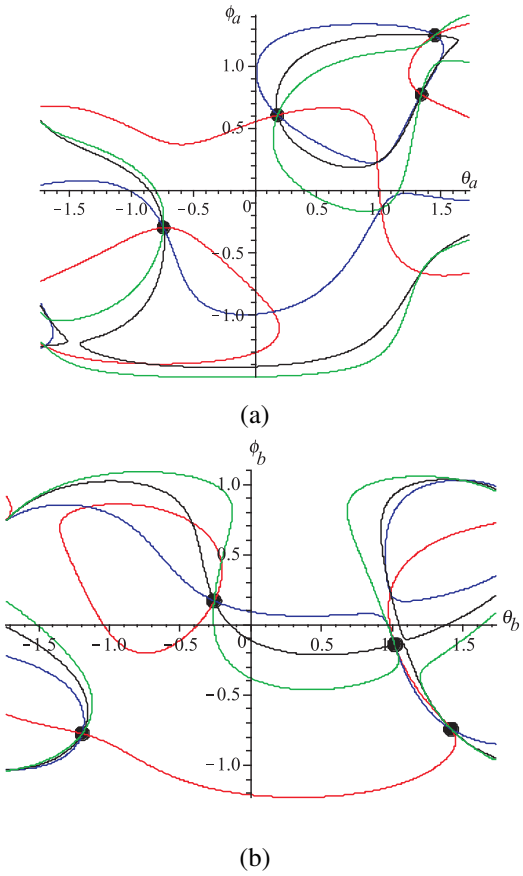

FIGURE 3. The four contours for Example 1 leading to four possible solutions: (a) for the moving axis, (b) for the fixed axis

TABLE 2. Solutions of Example 1

	$\mathbf{a}_0$(or $\mathbf{a}_0^\star$)	$\mathbf{b}$(or $\mathbf{b}^\star$)
# 1	$[0.7085, -.6418, -.2932]$	$[0.2640, -.6636, -.6998]$
# 2	$[0.0385, 0.3163, 0.9478]$	$[0.1143, 0.7263, -.6777]$
# 3	$[0.1642, 0.6977, 0.6972]$	$[0.5218, 0.8413, -.1403]$
# 4	$[0.8077, 0.1493, 0.5702]$	$[0.9524, -.2535, 0.1686]$

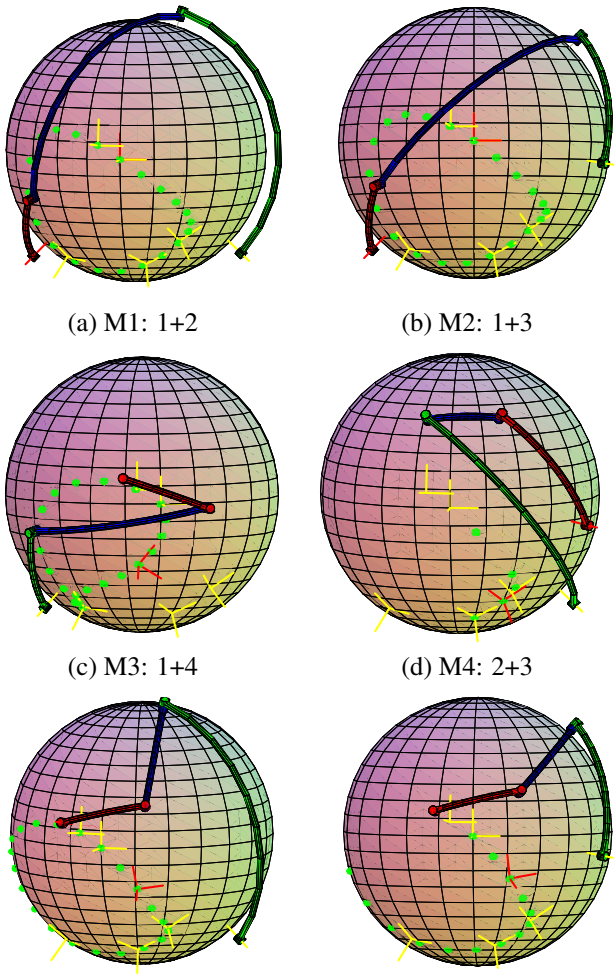

FIGURE 4. Six synthesized mechanisms shown together with all task orientations in yellow. The frames in red show the orientations of the coupler, while solid dots show some traces of the origin of this frame. Index 1+2 stands for a mechanism generated from the #1 and #2 solutions, and so on.

6.2 Example 2: Synthesis with Four Poses

In the case of four-pose synthesis, there are infinitively many solutions available, represented by the circlepoint and centerpoint curves. Taking the first four poses of Example 1, the circlepoint conical surface $\mathscr{K}$ was obtained for unit vector $\mathbf{a}_0 = [x, y, z]^T$ as

$$\begin{aligned} F(\mathbf{a}_0) = & -0.01766x^3 + 0.03116x^2y + 0.04156x^2z + 0.02939xy^2 \\ & + 0.08747xyz - 0.06021xz^2 - 0.01747y^3 - 0.02155y^2z \\ & + 0.02673yz^2 - 0.00482z^3 \end{aligned} \tag{26}$$

Copyright © 2010 by ASME

Likewise, the centerpoint conical surface $\mathscr{M}$ was obtained for unit vector $\mathbf{b} = [u, v, w]^T$ as

$$F(\mathbf{b}) = 0.01678\,u^3 + 0.05157\,u^2 v + 0.01743\,u^2 w - 0.04005\,uv^2 + 0.02803\,uvw - 0.05074\,uw^2 - 0.00259\,v^3 - 0.05317\,v^2 w - 0.00933\,vw^2 + 0.02762\,w^3 \quad (27)$$

The corresponding circlepoint and centerpoint curves are shown in Fig. 5. One of the two curves can be used to select two points. For example, we can select two centerpoints from the centerpoint curve. The corresponding circlepoints are then found form the intersection of the circlepoint curve with the three planes derived from linear equations (13). Apparently, infinitely many dyads are capable of visiting the prescribed orientations.

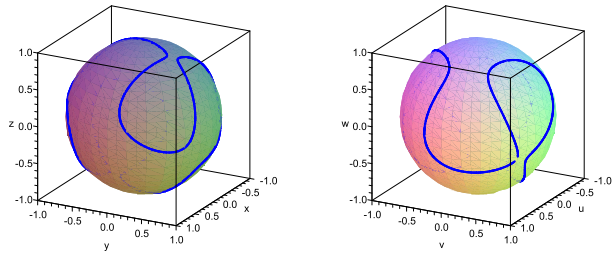

(a) (b)

FIGURE 5. Four-pose synthesis curves on the unit sphere, (a) the circlepoint curve and (b) the centerpoint curve

6.3 Example 3: Synthesis with a P-joint

In this example, the five prescribed attitudes are listed in Table 3. These attitudes, involve displacement, $\mathbf{c}_1, \ldots, \mathbf{c}_4$ that are coplanar, and hence, admit one fixed P-joint. We determine first the dyad comprising one P-joint. By using Eq. (25), contours of four determinant equations are plotted in Fig. 6. It is seen that there is only one solution $\{\vartheta_a, \varphi_a\}$. The corresponding unit vector $\mathbf{b}^\star$ is thus obtained, followed by the unit vector $\mathbf{a}_0$. For the remaining dyad consisting of two R-joints, four solutions are found with a procedure similar to that of Example 1. Of the four solutions of $\mathbf{a}_0$ and $\mathbf{b}$, one is identical to the solution of $\mathbf{a}_0^\star$ and $\mathbf{b}^\star$. In other words, solutions of the dyad containing one P-joint are a special case of the general spherical R-R dyad. All results are listed in Table 4.

Altogether, there are three possible mechanisms containing one P-joint for the given solutions. One synthesized mechanism is shown in Fig. 7, which is a branching-free mechanism, as made apparent by animations.

TABLE 3. Five poses for Example 3

ϕ_j[rad]	$\mathbf{e}^T$	$[\beta_1, \beta_2, \beta_3]$[deg]
0	[0,0,1]	[0,0,0]
0.2563	$[-0.2280, -0.4553, -0.8606]$	$[-12.5, 7.0, -2.6]$
1.1307	$[-0.0578, 0.2370, -0.9697]$	$[-64.2, -10.5, -10.8]$
1.1938	$[0.5049, 0.8505, -0.1468]$	$[14.3, -56.9, 45.6]$
1.3665	$[0.7119, 0.6601, 0.2393]$	$[45.1, -30.7, 73.2]$

TABLE 4. Solutions of Example 3

	$\mathbf{a}_0$	$\mathbf{b}$
# 1	$[0.2845, 0.3863, 0.8773]$	$[0.1219, -.7089, -.6946]$
# 2	$[0.7226, 0.5295, 0.4442]$	$[0.2309, 0.4566, 0.8591]$
# 3	$[0.9573, -.2433, 0.1555]$	$[0.8134, 0.1643, 0.5579]$
	$\mathbf{a}_0^\star$	$\mathbf{b}^\star$
# 4	$[0.5221, 0.8442, -.1208]$	$[0.0655, 0.1015, 0.9926]$

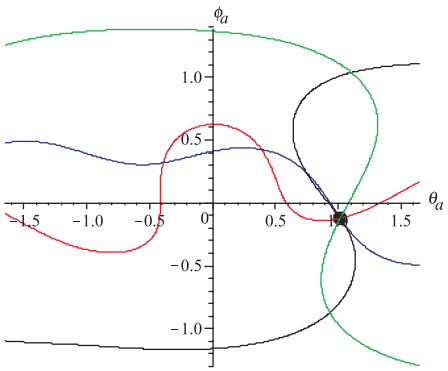

FIGURE 6. Contour plot to find position vectors for the unit vector of the P-joint.

7 Discussion and Conclusions

In this paper, the spherical Burmester problem was revisited with the intent of formulating not only a robust set of synthesis equations but also a robust solution of the equations thus resulting. Both are considered essential for mechanism synthesis.

The synthesis equations were formulated in the space of two independent angles, longitude and latitude, which led, for five prescribed poses, to a system of four overdetermined nonlinear equations in two unknowns. A semigraphical approach led to a visual estimation of the real solutions, which were then used as initial guesses to a Newton-Gauss procedure. The formulation is robust in that it is general enough, to account for the existence of spherical prismatic joints. Robustness in the

Copyright © 2010 by ASME

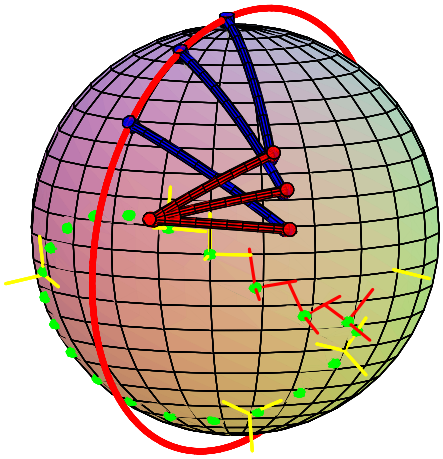

FIGURE 7. One synthesized mechanism with a P-joint, showing three link positions.

solution lies in the overdeterminency of the synthesis equations and the avoidance of roundoff-error propagation.

Branch-defect is detected by means of a sign-change in the sine of the transmission angle. All tasks are incorporated into one working platform developed on Maple, with the semigraphical approach, which aids in the visualization of the synthesis problem.

REFERENCES

[1] R.S. Hartenberg and J. Denavit. *Kinematic Synthesis of Linkages*. McGraw-Hill, New York, 1964.

[2] J.R. Zimmerman. Four-precision-point synthesis of the spherical four-bar function generator. *Journal of Mechanisms*, 2(1):133–139, 1967.

[3] C. H. Chiang. *Kinematics of Spherical Mechanism*. Cambridge University Press, Cambridge, 1988.

[4] J. M. McCarthy. *Geometric Design of Linkages*. Springer-Verlag, New York, 2000.

[5] K. Al-Widyan and J. Angeles. The synthesis of robust spherical motion generators. In *Proc. 2004 ASME Design Engineering Technical Conferences*, Lake City, Utah, 2006. DETC2004-57422.

[6] K. Brunnthaler, H.P. Schrocker, and M. Husty. Synthesis of spherical four-bar mechanisms using spherical kinematic mapping. In *Advances in Robot Kinematics,* J. Lennarcic and B. Roth. (editors), pages 377–384, Springer, Netherlands, 2006.

[7] L. Burmester. *Lehrbuch der Kinematik*. Arthur Felix Verlag, Leipzig, Germany, 1888.

[8] C. Chen, S. Bai, and J. Angeles. A comprehensive solution of the classic Burmester problem. *CSME Transactions*, 32(2):137–154, 2008.

[9] J. Angeles. *Fundamentals of Robotic Mechanical Systems*. Springer-Verlag, New York, 2002.

[10] G. Dahlquist and A. Bjorck. *Numerical Methods*. Prentice Hall, Englewood Cliffs, NJ, 1974.

[11] J. Angeles and A. Rojas. An optimisation approach to the branching problem of plane linkage synthesis. In *Proc. Sixth World Congress on the Theory of Machines and Mechanisms*, pages 120–123, Dec. 15–20, New Delhi, 1983.

[12] P. Zsombor-Murray. Kinematic mapping and kinematics of some parallel manipulators. In *Proc. of the Second Int. Workshop on Fundamental Issues and Future Research Directions for Parallel Mechanisms and Manipulators*, pages 41–48, September 21–22, Montpellier, France, 2008.

Copyright © 2010 by ASME